THE JOURNAL OF PHYSICAL CHEMISTRY B

Article

pubs.acs.org/JPCB

# Monte Carlo Study of Polyelectrolyte Adsorption on Mixed Lipid Membrane

Xiaozheng Duan,[†] Ran Zhang,[†] Yunqi Li,[‡] Tongfei Shi,*[,†] Lijia An,[†] and Qingrong Huang[‡]

[†]State Key Laboratory of Polymer Physics and Chemistry, Changchun Institute of Applied Chemistry, Chinese Academy of Sciences, Changchun, 130022, P. R. China

[‡]Food Science Department, Rutgers University, New Brunswick, New Jersey 08901, United States

Supporting Information

**ABSTRACT:** Monte Carlo simulations are employed to investigate the adsorption of a flexible linear cationic polyelectrolyte onto a fluid mixed membrane containing neutral (phosphatidyl-choline, PC), multivalent (phosphatidylinositol, $PIP_2$), and monovalent (phosphatidylserine, PS) anionic lipids. We systematically study the effect of chain length and charge density of the polyelectrolyte, the solution ionic strength, as well as the membrane compositions on the conformational and interfacial properties of the model system. In particular, we explore (i) the adsorption/desorption limit, (ii) the interfacial structure variations of the adsorbing polyelectrolyte and the lipid membrane, and (iii) the overcharging of the membrane. Polyelectrolyte adsorbs on the membrane when anionic lipid demixing entropy loss and polyelectrolyte flexibility loss due to adsorption are dominated by electrostatic attraction between polyelectrolyte and anionic lipids on the membrane. Polyelectrolytes with longer chain length and higher charge density can adsorb on the membrane with increased anionic lipid density under a higher critical ionic concentration. Below the critical ionic concentration, the adsorption extent increases with the charge density and chain length of the polyelectrolyte and decreases with the ionic strength of the solution. The diffusing anionic lipids prohibit the polyelectrolyte chain from forming too long tails. The adsorbing polyelectrolyte with long chain length and high charge density can overcharge a membrane with low charge density, and conversely, the membrane charge inversion forces the polyelectrolyte chain to form extended loops and tails in the solution.

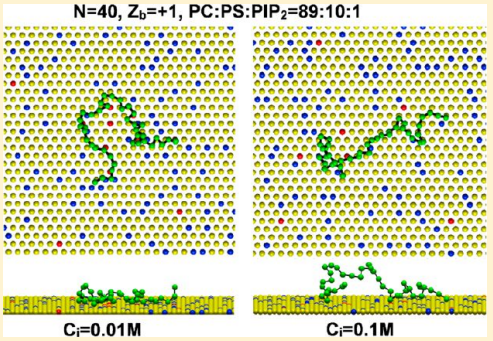


## 1. INTRODUCTION

Various cationic macromolecules can adsorb onto the plasma membranes and attract the laterally diffusing multivalent (i.e., phosphatidylinositol 4,5-bisphosphate, $PIP_2$, which comprises only 1% or less of all the membrane surface phospholipids) and monovalent (i.e., phosphatidylserine, PS, which comprises 10−20% of phospholipids) anionic lipids around to achieve local electrical neutrality.[1−3] This macromolecule/membrane adsorption interaction results in macromolecule conformational variations and corresponding anionic lipid segregation, which function in nearly all cell physiological activities including endocytosis, phagocytosis, ion channel activation, cytoskeletal attachment, vesicle trafficking, protein modulation in cancer, etc.[1,4−6]

Experimental investigations on adsorption between charged macromolecules and oppositely charged lipid membranes or liposomes have been extensively carried out via different experimental methods (e.g., neutron reflectivity, fluorescence microscopy, transmission electron microscopy, and X-ray)[7−20] as model systems for understanding the related mechanisms in life science[1,4−6,21] and biological applications, for instance, biosensors,[22−24] nanoreactors,[25] nanofluid devices,[26] protein chips,[27] food industry,[28] medical implants,[29,30] etc. It has been illustrated that "nonspecific electrostatics" between cationic macromolecules and anionic lipids in a membrane is the main drive for the adsorption mechanism.[1] Studies based on the lateral probe distribution demonstrated that the adsorption of cationic macromolecules or unstructured polypeptides can extensively cluster the anionic lipids[9,31−35] in a membrane and confine their diffusion.[1,2,17] Conversely, the responsive anionic lipids affect the adsorbing macromolecule's structure behavior and restrict its mobility.[3,36] Owing to the unstable physical and chemical states of the charged lipids and the lack of appropriate probes and approaches for the system detected in experimental studies,[1,30] effective theoretical calculation and computational modeling have also been extensively applied to further explore the static and kinetic behaviors of the macromolecule/membrane complex. The localization of bound charged lipids around the peripherally adsorbing macromolecules has been well addressed.[16,18,19] Atomic-level models[5,34] and statistical-thermodynamically associated approaches exploring the energetic−entropic balance of macromolecule electrostatic adsorption onto the lipid membranes[2,5,7,16,18,37] have been extensively proposed. Coarse-grained models, considering the

Received: October 10, 2012
Revised: December 18, 2012
Published: January 4, 2013

lipids within regular solution theory and the macromolecules as hard spheres[38] and linear polyelectrolyte,[39,40] have been employed to carefully investigate the charged macromolecule adsorption onto the membrane and the corresponding membrane lipid demixing. Other models considering the macromolecule as a homogeneous flat surface,[41] rectangles,[42] cylinders,[43] etc., have also provided instructive results for further understanding the extent of charged lipid clustering, the corresponding entropy loss and energy gain, and the lipid dynamic behaviors induced by adsorbate attraction.

For this macromolecule/membrane system, the interaction between the charged macromolecule and membrane sensitively depend on the chain properties of the charged macromolecule (such as the degree of polymerization and the charged density),[2] the ionic strength of the solution,[8] as well as the composition of the charged membranes.[39,44] The adsorbing macromolecules may contain various numbers of basic residues with positive charges, for instance, EGFR comprises 8 basic residues, GAP43 comprises 9 basic residues, and MARCKS comprises 13 basic residues, etc.[1] Polypeptides of lysine and arginine with various polymerization degrees are also widely used as models in the macromolecule/membrane system studies.[15,29,30,34,44] Generally, the physiological ionic strength ranges from ∼0.10 to ∼0.15 M,[45] which may vary slightly from different local physiological environments. Experimental investigations on the macromolecule/membrane system within other salt solution ionic strengths have also been carried out to further investigate the biophysical mechanism of the system,[8] which showed that minor variation of the solution ionic strength can sensitively influence the adsorption. As far as we are aware, until now, very few investigations have focused on the influence of the cooperativity effect and charge density variations of the macromolecules and solution screening effect on the detailed interfacial structures and conformational behaviors of the adsorbing cationic macromolecules, the corresponding demixing of the responsive diffusing charged lipids on mixed membrane, and the adsorption/desorption behaviors of the complex, which are fundamental problems to determine the static and kinetic behaviors of the whole complex as well as the related cellular activities.[1,4−6] Thus, systematical investigations on these issues cannot only help to further understand the biophysical processes but also help to develop relative disease therapy by regulating the macromolecule binding.[6]

To explore such problems quantitatively, in the present study, we employ Monte Carlo simulations to investigate the model of a flexible cationic polyelectrolyte interacting with membranes containing laterally mobile neutral, monovalent, and tetravalent anionic lipids in salt solutions in the equilibrium state. We analyze the effect of the chain length and charge density of polyelectrolyte, solution ionic strength, as well as membrane composition on the adsorption/desorption limit of the polyelectrolyte/membrane system, the adsorbing polyelectrolyte conformations and corresponding membrane interfacial structure, the surface coverage, the polyelectrolyte adsorption amount, and the overcharging of the membrane. Particularly, we characterize the conformations of the adsorbing chains by their loops, trains, and tails formed on the membrane surface. It is found that polyelectrolytes with longer chain length and higher charge density can adsorb on the membrane with increased anionic lipid density under a higher critical ionic concentration, below which the adsorption extent further increases with the charge density and chain length of the polyelectrolyte as well as the membrane charge density and decreases with the ionic strength of the solution. Multivalent lipids preferentially bind around the polyelectrolyte and competitively inhibit the binding of monovalent lipids, and the responsive diffusing anionic lipids prohibit the polyelectrolyte chain from forming long tails. The membrane charge inversion induced by polyelectrolyte adsorption and the corresponding chain conformational variations are also discussed. We hope our systematic work can offer a perspective to further interpret the biological mechanism of the macromolecule/membrane system that has been studied extensively over the decades in more complicated systems, and give some further inspiration in biophysics and medical implication.

The paper is organized as follows. We first depict the computational method of Monte Carlo simulation, including molecular models, simulation details, and the calculated properties. Then, we present our numerical results and discussion on the adsorption/desorption limit, polyelectrolyte conformational variations, and the corresponding anionic lipid rearrangement as well as the overcharging of the membrane. Finally, the conclusion is addressed. Some data not shown are given in the Supporting Information.

## 2. SIMULATION METHOD

**2.1. Model.** In our work, we employ Monte Carlo simulation to investigate the interaction between a single flexible cationic polyelectrolyte and a fluid mixed membrane in the equilibrium state. Our model is constructed on the basis of a previous study[39] with minor modifications.

We employ a flat and impenetrable two-dimensional hexagonal lattice surface to model the binary or ternary mixed lipid membranes, composed of electrically neutral ($Z_l$ = 0), monovalent ($Z_l$ = −1), and tetravalent ($Z_l$ = −4) lipid headgroups, which represent the phosphatidyl-choline (PC), phosphatidylserine (PS), and phosphatidylinositol 4,5 bisphosphate ($PIP_2$) lipids mentioned in the previous section, respectively. Totally, 50 × 50 = 2500 lipid headgroups reside at all lattice sites on the membrane layer. The lipid headgroups on the membrane could be considered as a hexagonal array of closely packed disks with a diameter of $d$ = 8.66 Å, and each lipid headgroup's area is set as 65 Å$^2$. Focusing on the problems of biological interest, we mainly explore polyelectrolyte adsorption/desorption on a membrane with four types of representative compositions, which are PC:PS:$PIP_2$ = 98:1:1, PC:PS:$PIP_2$ = 89:10:1, PC:$PIP_2$ = 99:1, and PC:PS = 90:10, respectively. The lipid charges (equal to $Z_l$) are regarded as point charges residing at the grid points on the hexagonal lattices.

A freely jointed chain with $N$ connected hard spheres is employed to model the polyelectrolyte chain.[46] Each sphere represents a physical bead with radius $\sigma_b$ = 4.33 Å and one or two positive charges equal to $Z_b$ residing at the bead center. The fraction of ionized beads is set as ,1 and the bond length is constant and equal to the membrane lattice constant $d$ (8.66 Å).

The total energy $U$ ($k_BT$ units) of the system can be written as

$$U = U_{unbond} + U_{bond} + U_{angle} \quad (1)$$

The polyelectrolyte is a freely flexible chain; thus, $U$ is free of the angle energy

$$U_{angle} = 0 \quad (2)$$


dx.doi.org/10.1021/jp310017j | J. Phys. Chem. B 2013, 117, 989−1002

In eq 1, the nonbonding energy is a summation of the hard sphere repulsion and Coulomb interaction

$$U_{\text{unbond}} = U_{\text{H-S}} + U_{\text{Coul}} \tag{3}$$

The hard sphere repulsion ($U_{\text{H-S}}$) is employed between impenetrable membrane and the polyelectrolyte and between beads of the polyelectrolyte. $U_{\text{H-S}}$ has a positive infinite value if the distance between two bead centers is less than $d$ or the distance between any bead center and the membrane surface is less than $d/2$; otherwise, it has a value of 0.

The Coulomb interactions ($U_{\text{Coul}}$), including the electrostatic repulsion between beads of the polyelectrolyte, the electrostatic repulsion between anionic lipids, and the electrostatic attraction between anionic lipids and beads of the polyelectrolyte, are calculated via the Debye−Hückel (DH) approximation, an approximation widely used for electrostatic interaction quantification in similar systems,[39,47] in units of $k_BT$

$$u_{\text{el}}(r_{ij}) = Z_i Z_j l_B \frac{\exp(-\kappa r_{ij})}{r_{ij}} \tag{4}$$

where $Z_i$ and $Z_j$ are the amount of charge on particles (polyelectrolyte beads or lipid headgroups) $i$ and $j$ with a distance of $r_{ij}$. The Bjerrum length

$$l_B = \frac{e^2}{4\pi\varepsilon_r\varepsilon_0 k_B T} \tag{5}$$

where $e$ is the elementary charge ($1.6 \times 10^{-19}$ C), $\varepsilon_0$ is the vacuum dielectric permittivity ($8.854 \times 10^{-12}$ C V$^{-1}$ m$^{-1}$), and $k_B$ is the Boltzmann constant ($1.3807 \times 10^{-23}$).

The polyelectrolyte and lipid monolayer immerse in salt solution, which contains a symmetric 1:1 electrolyte with concentration $C_i$. The relative dielectric constant of the solvent $\varepsilon_r$ ($\varepsilon_s$), taken as that of water at 298 K, is fixed at 78.5, and the dielectric constant of the membrane interior $\varepsilon_r$ ($\varepsilon_m$) is set as 2.[44,47] Free ions are not explicitly included in the model, and their overall effect is calculated via the dependency of the inverse Debye screening length $\kappa^2$ (m$^{-2}$) on the electrolyte concentration

$$\kappa^2 = 1000 e^2 N_A \sum_i \frac{Z_i^2 C_i}{\varepsilon_0 \varepsilon_r k_B T} \tag{6}$$

where $N_A$ is Avogadro's number ($6.022 \times 10^{23}$ mol$^{-1}$) and $C_i$ is the solution ionic concentration (mol L$^{-1}$). For a simple description, we utilize $k_BT$ as the energy unit and $d$ as the distance unit unless specific notification.

**2.2. Simulation Details.** In the calculations, we perform the Monte Carlo simulations in the NVT (constant particle numbers, constant volume, and temperature) ensemble according to the Metropolis algorithm,[48] in which successive "trial" configurations are generated to sample the low-energy conformations. The two-dimensional periodical boundary condition is adopted in the $x$ and $y$ directions, and the $z$ direction is infinite.

On the mixed membrane, we employ Kawasaki moves[49,50] to sample new anionic lipid conformations by swapping the anionic lipids with randomly selected neighbors. For the polyelectrolyte, to relax the chains effectively and accelerate the convergence of energy, several algorithms including kink-jump, crankshaft, translation, and pivot are employed.[51] Thus, a complete time step of the simulation consists of the following consecutive operations: (i) all anionic lipids on the membrane attempt a random movement; (ii) all beads of the polyelectrolyte attempt a movement. The trial move sequences of lipids and polyelectrolyte beads are generated randomly, which are accepted with a Metropolis rule with the acceptation probability of $W = 1$ if $E_1 \le E_0$ and $W = e^{-(E_1-E_0)/k_BT}$ if $E_1 \ge E_0$, in which $E_0$ and $E_1$ are the energies of the "old" and "new" system states, respectively. If the trial movement is accepted, the complex promotes to the "new" configuration; if rejected, the bead of polyelectrolyte or lipid remains at its previous position.

At the beginning of the simulations, we randomly generate the anionic lipids on the lattice sites of the membrane and put the polyelectrolyte chain with randomly generated conformation onto the membrane surface. Then, the $1 \times 10^6$ MC step athermal relaxation starts, and in this process, the polyelectrolyte is controlled to relax in the Debye screening length range above the membrane, which can only interact with the membrane via $U_{\text{H-S}}$. After the athermal relaxation, the polyelectrolyte starts to interact with the anionic lipids on the membrane with $U_{\text{H-S}}$ and $U_{\text{DH}}$ for another $2 \times 10^6$ MC steps which we have tested long enough to achieve energy minimization and equilibrium of the system. Then, we examine the system in another $2 \times 10^6$ MC steps for the ensemble average. In summary, each simulation run includes $1 \times 10^6$ MC steps for athermic relaxation, $2 \times 10^6$ MC steps for equilibration, and another $2 \times 10^6$ MC steps for the ensemble average and results collection. We carry out 20 parallel simulations with different random seeds for each system, and give the ultimate average results in the paper.

To investigate the influence of chain length and charge density of the polyelectrolytes on the adsorption/desorption and conformational changes in the polyelectrolyte/membrane system, we vary the number of polyelectrolyte beads ($N$) from 10 to 100 and set the charge densities ($Z_b$) of polyelectrolytes as +1 and +2. In addition, to explore the screening effect of salt solution, the solution ionic concentration in eq 6 ranges from $C_i = 0.001$ M ($\kappa^{-1} = 96$ Å) to $C_i = 1$ M ($\kappa^{-1} = 3$ Å), which can cover the scopes of physiological and experimental ionic strengths.

**2.3. Calculated Properties.** We calculate several properties to analyze the polyelectrolyte conformations, bead positions on the membrane surface, and corresponding redistribution of anionic lipids in the membrane. We collect the results every 1000 Monte Carlo steps during the simulation, and calculate the ensemble averages (denoted by $\langle\ \rangle$) of these properties for $2 \times 10^6$ MC steps of equilibration.

The mean-square radius of gyration ($\langle R_g^2 \rangle$) and its components orthogonal ($\langle R_g^2 \rangle_O$) and parallel ($\langle R_g^2 \rangle_P$) to the membrane surface are calculated to describe the anisotropic shape variations of the polyelectrolyte

$$\langle R_g^2 \rangle = \frac{1}{N} \sum_i^N \langle (r_{\text{cm}} - r_i)^2 \rangle \tag{7}$$

$$\langle R_g^2 \rangle_O = \frac{1}{N} \sum_i^N \langle (z_{\text{cm}} - z_i)^2 \rangle \tag{8}$$

$$\langle R_g^2 \rangle_P = \frac{1}{N} \sum_i^N \langle (y_{\text{cm}} - y_i)^2 \rangle + \langle (x_{\text{cm}} - x_i)^2 \rangle \tag{9}$$

where $r_{\text{cm}}$ is the position of the mass center of the polyelectrolyte chain and $x_{\text{cm}}$, $y_{\text{cm}}$, and $z_{\text{cm}}$ are the


dx.doi.org/10.1021/jp310017j | J. Phys. Chem. B 2013, 117, 989−1002

Table 1. Equilibrated Structures of the Polyelectrolyte/Membrane Complex as a Function of $N$, $Z_b$, and $C_i$[a]

| $N(Z_b)$ \ $C_i$[M] | 0.001 | 0.01 | 0.03 | 0.06 | 0.1 | 1 |
|---|---|---|---|---|---|---|
| 10(+1) | 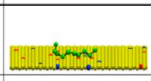 | 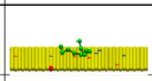 | 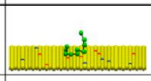 | 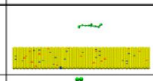 | 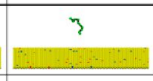 | 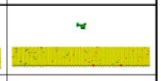 |
| 20(+1) |  | 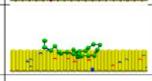 | 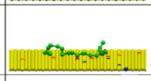 | 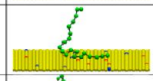 | 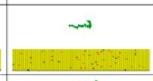 | 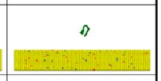 |
| 40(+1) | 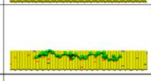 | 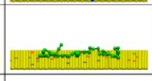 | 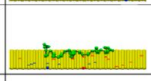 | 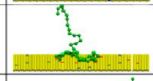 | 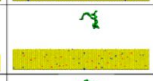 |  |
| 60(+1) | 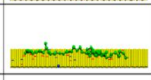 | 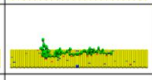 | 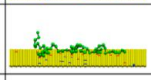 | 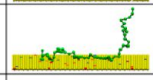 | 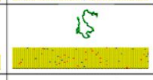 | 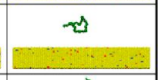 |
| 80(+1) | 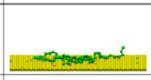 | 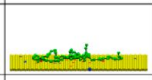 | 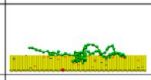 | 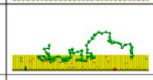 | 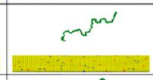 | 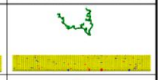 |
| 100(+1) | 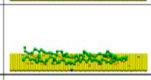 | 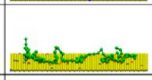 | 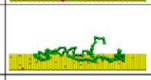 | 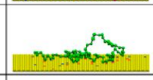 | 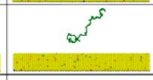 | 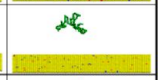 |
| 10(+2) | 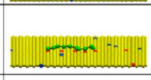 | 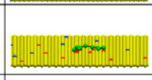 | 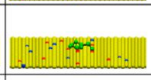 | 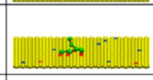 |  |  |
| 20(+2) |  |  |  |  |  |  |
| 40(+2) |  |  |  |  |  |  |
| 60(+2) |  |  |  |  |  |  |
| 80(+2) |  |  |  |  |  |  |
| 100(+2) |  |  |  |  |  |  |

[a]The membrane compositions are PC:PS:$PIP_2$ = 98:1:1.

corresponding Cartesian coordinates; $r_i$ is the mass center of the $i$th polyelectrolyte bead, and $x_i$, $y_i$, and $z_i$ are its Cartesian coordinates.

The membrane surface locates in the $x-y$ plane, which is orthogonal to the $z$ axis at $z = 0$. To analyze the position of the polyelectrolyte chain beads on the membrane surface, we define several layers parallel to the membrane surface. Each layer's thickness is set as one bead radius $\sigma_b$ (4.33 Å). Due to the excluded volume effect, polyelectrolyte beads' centers can never visit the adjacent layer of one bead's radius (4.33 Å) in thickness; thus, the thickness of the first layer is set as one bead diameter (8.66 Å). To describe the structure of the adsorbing polyelectrolyte, we calculate the number of beads of the polyelectrolyte in trains, loops, and tails, which describe different conformations of the polyelectrolyte chain adsorbing onto the membrane surface: a train indicates connected beads lying in heights less than $d$ (8.66 Å) on the membrane surface, a loop indicates beads between two neighbor trains but rises up from the membrane surface, and a tail denotes contiguous beads extending into the solution but does not return into the range less than $d$ on the membrane.[52]

We define membrane surface coverage as the fraction of the membrane surface covered by the polyelectrolyte beads adsorbing in the first layer

$$\theta = \frac{\alpha_0 N^*}{\alpha_{surf}} \tag{10}$$

Here $a_0$ is the projected area of each polyelectrolyte bead, $N^*$ is the number of adsorbing beads in the first layer, and $a_{surf}$ represents the membrane surface area.

The polyelectrolyte adsorption amount $\Gamma$ on the membrane is defined as

$$\Gamma = \theta/\theta_{max} \tag{11}$$

in which $\theta_{max} = Na_0/a_{surf}$ is the maximum surface coverage of the membrane covered by a completely adsorbing polyelectrolyte.

We also define the "electronic adsorption amount", $\Gamma_e$, as

$$\Gamma_e = Z_b N^*/Q_m \tag{12}$$

where $Q_m$ is the total charge amount of the anionic lipids in the mixed membrane. If $\Gamma_e > 1$, the total charge amount of the polyelectrolytes adsorbing within the first layer overcharges the membrane, which can induce the charge inverse of the membrane.

We employ the radial distribution functions (RDFs) to characterize the two-dimensional lipid distribution of each anionic lipid species. The RDF is the ratio between the average local concentration of other congeneric lipids at distance $r$ from each single lipid, and the average (or bulk) concentration of this lipid species in the membrane. RDFs can measure the variation in local lipid composition induced by polyelectrolyte adsorption.


dx.doi.org/10.1021/jp310017j | J. Phys. Chem. B 2013, 117, 989−1002

## 3. RESULTS AND DISCUSSION

When the cationic polyelectrolyte adsorbs onto the mixed membrane, the anionic lipids migrate toward and segregate around it to achieve local electrical neutrality. In Table 1, we present the equilibrated structures of the polyelectrolyte/membrane complex against polyelectrolyte chain length $N$, bead charge density $Z_b$, and solution ionic strength $C_i$. The membrane compositions are PC:PS:$PIP_2$ = 98:1:1.

**3.1. Adsorption/Desorption Limit.** We first detect the adsorption/desorption limit of the polyelectrolyte on the membrane. If the polyelectrolyte chain is in contact with the mixed membrane for more than half of the simulation time, we regard it as adsorbed. The solution ionic strength at the adsorption/desorption limit is defined as the critical solution ionic concentration ($C_i^C$). We adjust the solution ionic concentration ($C_i$) for cationic polyelectrolytes with different chain lengths ($N$) and charge densities ($Z_b$), interacting with four representative oppositely charged mixed membrane (PC:$PIP_2$ = 99:1, PC:PS:$PIP_2$ = 98:1:1, PC:PS:$PIP_2$ = 89:10:1, and PC:PS = 90:10), and plot $C_i^C$ against $N$, $Z_b$, and membrane compositions in Figure 1.

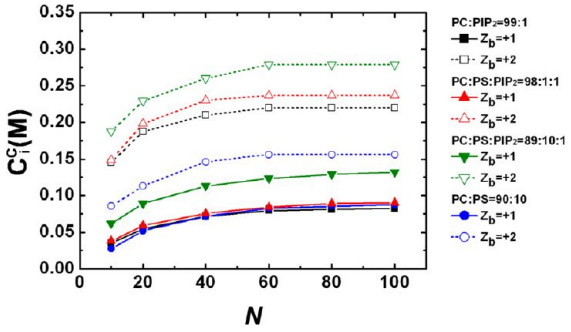


**Figure 1.** The critical ionic concentration $C_i^C$ (solution ionic strength at the adsorption/desorption limit) as a function of $N$, $Z_b$ in system with different membrane compositions.

When the charge density ($Z_b$) of the adsorbing polyelectrolyte is fixed as +1 (the solid symbols and solid lines), $C_i^C$ of the polyelectrolyte is relatively low. We first consider the adsorption/desorption limit of the cationic polyelectrolyte onto a binary mixed membrane (PC:$PIP_2$ = 99:1, the solid square symbols and solid lines). The solution ionic concentration is adjusted from 0.001 to 1 M for each polyelectrolyte with a chain length of $N$. With $N$ increasing from 10 to 100, the cooperativity effect of the network formed by the increased polyelectrolyte beads is enhanced. The $C_i^C$ increases with $N$ from 0.035 M ($N$ = 10) to 0.089 M ($N$ = 100). When the chain lengths are longer than 60 beads, $C_i^C$ gradually increases to reach a plateau close to 0.083 M. This means that, to dominate over the entropy loss of the polyelectrolyte conformation and loss of lipid freedom due to adsorption, stronger electrostatic attractions, with decreasing $C_i^C$, are required for shorter polyelectrolyte chain adsorption. We then investigate $C_i^C$ of the polyelectrolyte adsorbing onto a ternary mixed membrane with the composition of PC:PS:$PIP_2$ = 98:1:1 (the solid triangle symbols and solid lines), which contains 1% more monovalent PS lipids than the binary mixed membrane (PC:$PIP_2$ = 99:1). The increased total charge density of the membrane caused by addition of the PS anionic lipids leads to slightly stronger attraction between the membrane and polyelectrolyte, with a slight increase of $C_i^C$ than that of the membrane with PC:$PIP_2$ = 99:1. This is because, when the polyelectrolyte interacts with membrane, the increased charge density of the membrane reduces the demixing entropy loss of the anionic lipids due to adsorption; thus, the membrane can adsorb the polyelectrolyte under a higher $C_i^C$. With $N$ increasing from 10 to 100, $C_i^C$ increases from 0.038 to 0.090 M. When the membrane compositions are PC:PS:$PIP_2$ = 89:10:1 (the solid inverse triangle symbols and solid lines), the charge density on the fluid membrane is significantly increased by the additional pools of monovalent PS lipids, which greatly enhance the attraction between the membrane and polyelectrolyte. $C_i^C$ increases from 0.062 M ($N$ = 10) to 0.132 M ($N$ = 100). For the membranes with compositions of PC:PS = 90:10 (the solid round symbols and solid lines), each monovalent PS lipid carries only one charge; thus, the relatively weak electrostatic interaction between the anionic lipids and polyelectrolyte with short chain length and the relative higher demixing entropy loss of PS lipids[39] results in relatively lower $C_i^C$. With the increase of $N$, the increasing cooperativity effect of the polyelectrolyte enhances its interaction with the pool of monovalent PS lipids, leading to the increase of $C_i^C$.

When the charge density ($Z_b$) of the adsorbing polyelectrolyte is +2 (the vacant symbols and short dashed lines), electrostatic attractions between polyelectrolyte and membrane become stronger; thus, as shown in Figure 1, $C_i^C$ of a polyelectrolyte adsorbing onto a membrane with different lipid compositions increases significantly. Electrostatic attractions between polyelectrolyte beads with high charge density and multivalent $PIP_2$ lipids in the membrane increase more dramatically, and higher $C_i^C$ are required for the polyelectrolyte desorption from membrane containing $PIP_2$. In comparison, $C_i^C$ for a membrane with compositions of PC:PS = 90:10 presents quite lower values (the vacant round symbols and short dashed lines).

To sum up, adsorption is achieved when the attractive energy can dominate over the anionic lipid demixing entropy loss and polyelectrolyte flexibility loss. A stronger cooperative effect and electrostatic interaction from the beads of the polyelectrolyte with longer chain length and higher charge density, as well as the presence of multivalent charge lipids in the membrane, enable the polyelectrolyte chain to preferentially adsorb on the mixed membrane under a higher critical ionic concentration.

**3.2. Redistributions of the Anionic Lipids.** On the naked membrane with no polyelectrolyte adsorption, the electrostatic repulsions between the anionic lipids prohibit their aggregation; thus, the anionic lipids feely disperse on the membrane. The adsorption of polyelectrolyte can attract the anionic lipids and induce the lipid heterogeneity on the membrane. We employ the radial distribution functions (RDFs) to characterize the two-dimensional anionic lipid redistribution induced by polyelectrolyte adsorption. We plot the RDF variations of $PIP_2$−$PIP_2$ systems and PS−PS systems, denoted by $g_{PIP2-PIP2}(r)$ and $g_{PS-PS}(r)$, respectively, on the membrane with PC:PS:$PIP_2$ = 98:1:1 as a function of $C_i$ during the adsorption/desorption process. The ionic concentration of the solution ranges from $C_i$ = 0.001 M ($\kappa^{-1}$ = 96 Å), $C_i$ = 0.01 M ($\kappa^{-1}$ = 30 Å), $C_i$ = 0.03 M ($\kappa^{-1}$ = 18 Å), $C_i$ = 0.06 M ($\kappa^{-1}$ = 13 Å), $C_i$ = 0.1 M ($\kappa^{-1}$ = 10 Å), $C_i$ = 0.3 M ($\kappa^{-1}$ = 6 Å), to $C_i$ = 1 M ($\kappa^{-1}$ = 3 Å).

We first investigate the RDFs of each anionic lipid species in the membrane with a lipid composition of PC:PS:$PIP_2$ = 98:1:1. Parts a and b of Figure 2 show the variations of $g_{PIP2-PIP2}(r)$ and $g_{PS-PS}(r)$ on the naked membrane, respec-


dx.doi.org/10.1021/jp310017j | J. Phys. Chem. B 2013, 117, 989−1002

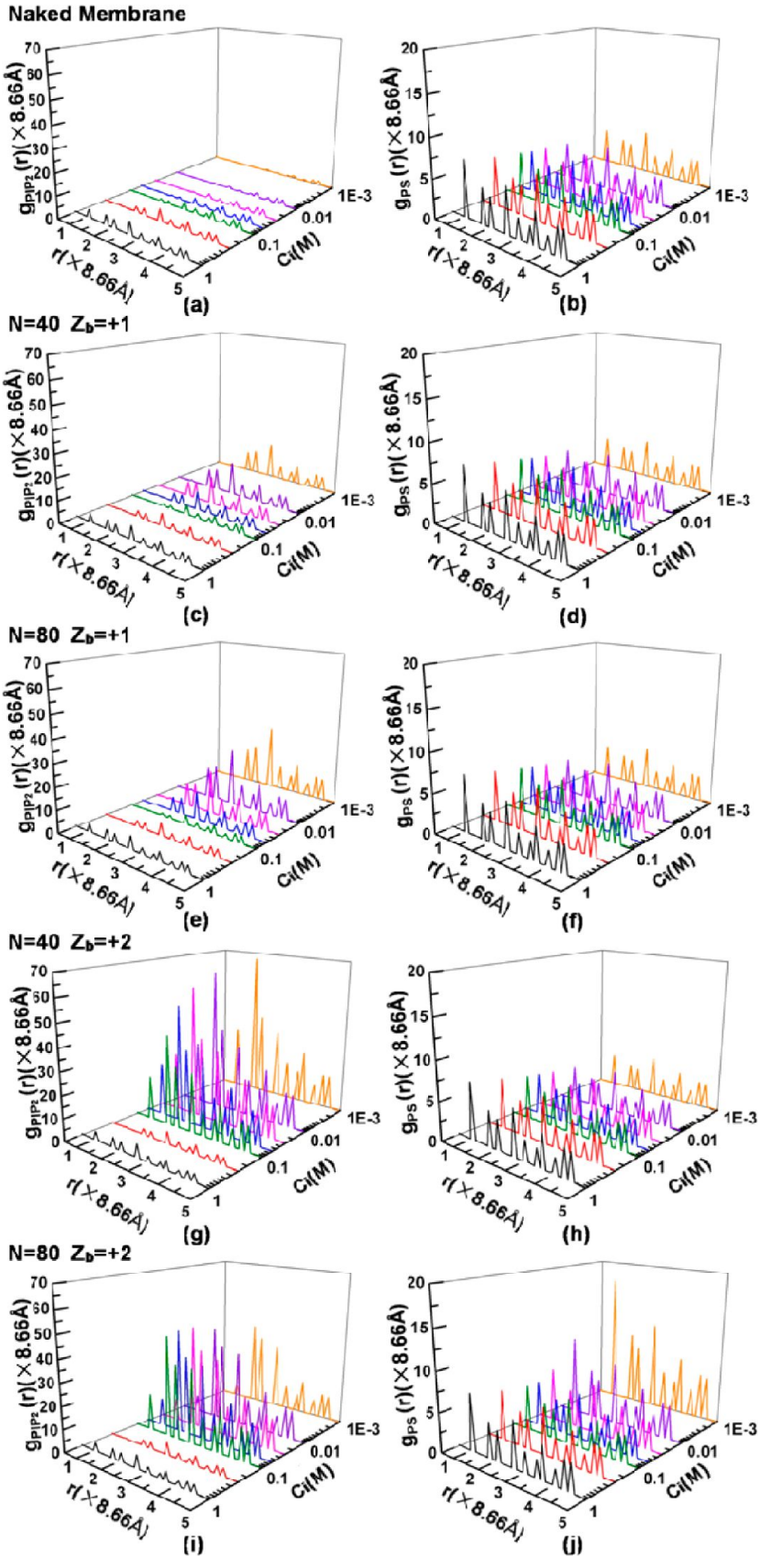


**Figure 2.** Radial distribution functions between the $PIP_2$ lipids and between the PS lipids as a function of solution ionic strength $C_i$. The membrane compositions are PC:PS:$PIP_2$ = 98:1:1. (a, b) Naked membrane. (c, d) $N$ = 40, $Z_b$ = +1. (e, f) $N$ = 80, $Z_b$ = +1. (g, h) $N$ = 40, $Z_b$ = +2. (i, j) $N$ = 80, $Z_b$ = +2.


dx.doi.org/10.1021/jp310017j | J. Phys. Chem. B 2013, 117, 989−1002

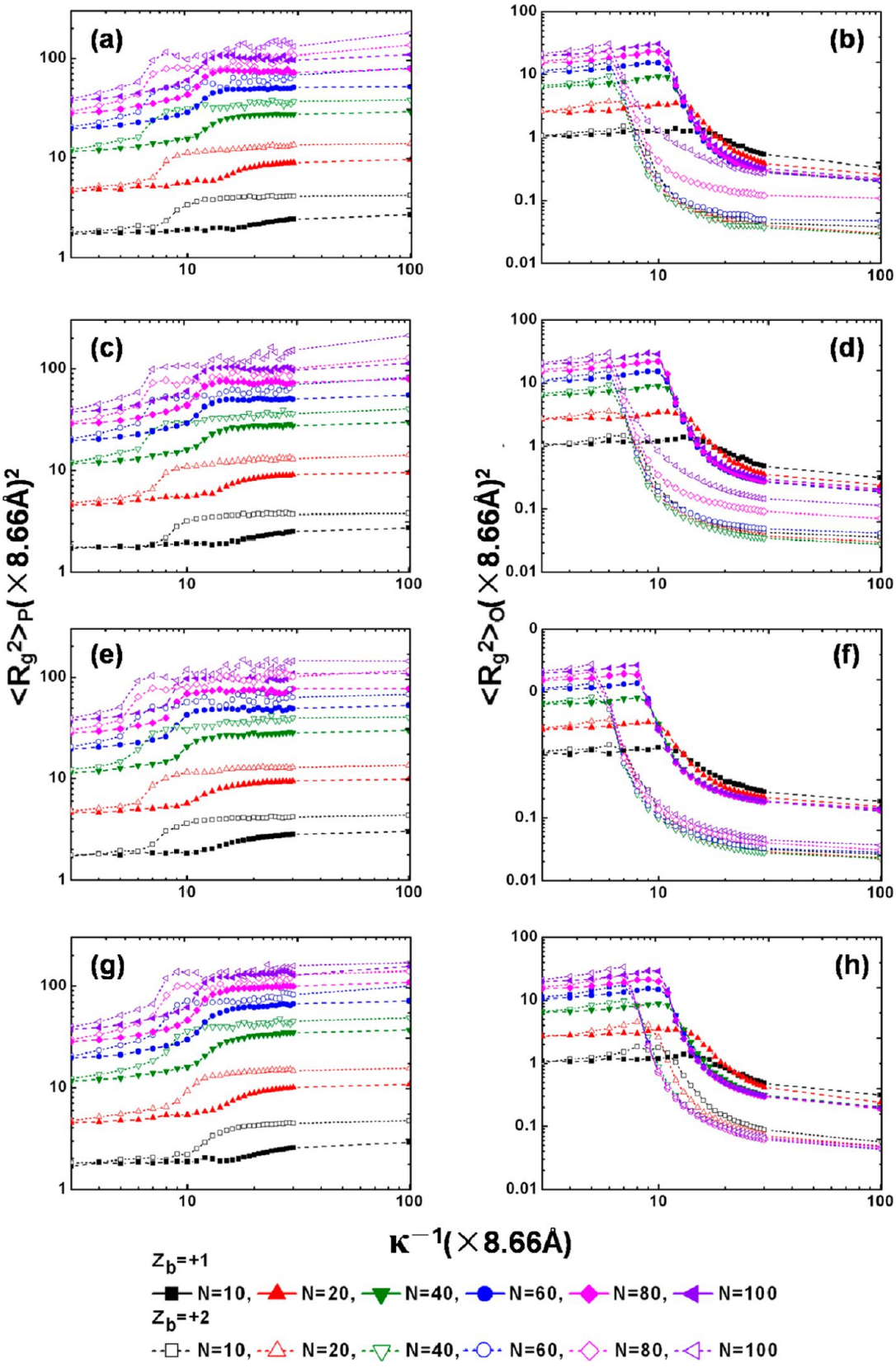


**Figure 3.** The orthogonal and parallel components of the mean-square radius of gyration, denoted as $\langle R_g^2 \rangle_P$ and $\langle R_g^2 \rangle_O$, respectively, as a function of $\kappa^{-1}$ at various chain lengths $N$ (from 10 to 100) and charge density $Z_b$ (+1 and +2). The membrane compositions are PC:PIP$_2$ = 99:1 (a, b), PC:PS:PIP$_2$ = 98:1:1 (c, d), PC:PS:PIP$_2$ = 89:10:1 (e, f), and PC:PS=90:10 (g, h).

tively, in the solution with different $C_i$. In both figures, with the increase of $C_i$ from 0.001 to 1 M, the increasing electrostatic screening effect of the solution weakens the electrostatic repulsion between the anionic lipids, leading to the increases of


dx.doi.org/10.1021/jp310017j | J. Phys. Chem. B 2013, 117, 989−1002

$g_{PIP2-PIP2}(r)$ and $g_{PS-PS}(r)$ at small $r$ ($r < 5$). Figure 2c shows $g_{PIP2-PIP2}(r)$ variations induced by polyelectrolyte adsorption ($N = 40$, $Z_b = +1$). When $C_i = 0.001$ M, a peak begins to appear in $g_{PIP2-PIP2}(r)$ at $r$ which is a little larger than 1.7, and the highest peak appears at $r$ which is larger than 2.5. This segregation is due to the attraction acting on the $PIP_2$ lipids by the electrostatic field emanating from the polyelectrolyte. By increasing $C_i$ to the critical adsorption/desorption limit $C_i^C$ (0.072 M), the peaks at small $r$ decrease gradually. This is because the increasing $C_i$ results in a stronger electrostatic screening effect of the solution, which weakens the attraction between the cationic polyelectrolyte and the anionic $PIP_2$ lipids in the membrane. When $C_i = 0.1$ M ($C_i > C_i^C$), the polyelectrolyte desorbs from the membrane and the $g_{PIP2-PIP2}(r)$ value at small $r$ rapidly decreases. By further increasing $C_i$ to 1 M, the polyelectrolyte chain diffuses away from the membrane and $g_{PIP2-PIP2}(r)$ at small $r$ increases significantly, which is in accordance with the corresponding results of naked membrane (see Figure 1a). Our results are consistent with previous experiments showing that the $PIP_2$ segregation decreases as the salt concentration increases.[8] As the chain length ($N$) of the polyelectrolyte increases to 80 beads (see Figure 2e), in the solution with $C_i < C_i^C$, the peaks increase significantly. This is because more $PIP_2$ lipids are required to segregate around the longer adsorbing polyelectrolyte to neutralize its cations. With $C_i$ increasing to the critical adsorption/desorption limit $C_i^C$, the polyelectrolyte desorbs from the membrane. In Figure 2g, when the charge density ($Z_b$) of the polyelectrolyte is +2 and the chain length ($N$) is 40 beads, in the solution with $C_i = 0.001$ M, peaks begin to appear in $g_{PIP2-PIP2}(r)$ at $r$ which is near 1, and the highest peak appears at $r$ which is slightly larger than 1.7. The increased peak values at small $r$ mean that a larger number of $PIP_2$ lipids compactly segregate underneath the adsorbing polyelectrolyte with higher charge density (+2). By further increasing $C_i$ to 0.3 ($C_i > C_i^C$), the polyelectrolyte desorbs from the membrane.

In comparison, parts d, f, and h of Figure 2 show the corresponding $g_{PS-PS}(r)$ values in these systems. We can observe that the $g_{PS-PS}(r)$ results in these three figures are quite similar to that of naked membrane (Figure 2b). With $C_i$ increasing from 0.001 to 1 M, a stronger electrostatic screening effect of the solution weakens the electrostatic repulsion between the monovalent PS lipids, leading to the increase of $g_{PS-PS}(r)$ at small $r$, but no significant change of $g_{PS-PS}(r)$ induced by the polyelectrolyte adsorption can be observed. The above RDF variations indicate that, in these cases, the $PIP_2$ lipid species preferentially bind around the polyelectrolyte in the adsorption/desorption process, whereas the PS lipids only function to minify the demixing entropy loss of the multivalent $PIP_2$ lipids in adsorption but do not directly interact with the polyelectrolyte and diffuse freely on the membrane. Thus, the $g_{PS-PS}(r)$ results remain the same as those in Figure 2b.

Parts i and j of Figure 2 show $g_{PIP2-PIP2}(r)$ and $g_{PS-PS}(r)$, respectively, induced by the adsorption of polyelectrolyte with $N = 80$ and $Z_b = +2$. When $C_i < 0.1$ M, $g_{PIP2-PIP2}(r)$ peaks at small $r$ in Figure 2i are lower than corresponding values in Figure 2g, whereas the corresponding $g_{PS-PS}(r)$ peaks in Figure 2j are higher than Figure 2h. The reason for these anionic lipid redistribution variations is that each multivalent $PIP_2$ lipid with four charges can incur a smaller demixing entropy loss and larger free energy gain in adsorption;[39] thus, the adsorbing polyelectrolyte preferentially segregates the multivalent $PIP_2$ lipids. When the polyelectrolyte's total charge amount ($Z_b \times N$) exceeds the $PIP_2$ lipids' total charge amount ($-4 \times 25 = -100$), it can bind all of these multivalent lipids. The enhanced cooperativity effect of the polyelectrolyte and electrostatic interaction cooperate to trap the $PIP_2$ lipids in a relatively incompact way along the longer linear polyelectrolyte. Simultaneously, the PS lipids are required to cluster around the polyelectrolyte−$PIP_2$ complex and neutralize the complex's surplus cations to achieve local charge neutralization. With the increase of $C_i$ from 0.001 M to $C_i^C$, the stronger electrostatic screening effect of the solution weakens the electrostatic repulsion between the mutivalent $PIP_2$ lipids and the electrostatic attraction between the polyelectrolyte beads and the monovalent PS lipids more significantly; thus, the $PIP_2$ lipids segregate more compactly and some binding PS lipids begin to escape from the complex, leading to a slight increase of $g_{PIP2-PIP2}(r)$ and a dramatic decrease of $g_{PS-PS}(r)$ at small r. Then, by further increasing $C_i$ to 0.3 M, the segregated multivalent $PIP_2$ lipids escape from the polyelectrolyte's control. The polyelectrolyte diffuses away from the membrane and the anionic lipids exhibit the original distribution in the naked membrane.

We also investigate RDFs of each lipid species in the membrane with lipid compositions of PC:PS:$PIP_2$ = 89:10:1, PC:$PIP_2$ = 99:1, and PC:PS:$PIP_2$ = 90:10. In the system with PC:PS:$PIP_2$ = 89:10:1 (see Figure S1 in the Supporting Information), the results of $g_{PIP2-PIP2}(r)$ and $g_{PS-PS}(r)$ are similar to those in Figure 2 (PC:PS:$PIP_2$ = 98:1:1). When the polyelectrolyte's cations are not enough to neutralize the multivalent anionic $PIP_2$ lipids, the polyelectrolyte preferentially segregates the $PIP_2$ lipids; when the polyelectrolyte's total charge amount is larger than that of $PIP_2$ lipids, it segregates all $PIP_2$ lipids and further attracts monovalent PS lipids. Because of the stronger background effect caused by the much larger average (or bulk) concentration of PS lipid species (10% of all lipids), the $g_{PS-PS}(r)$ peak values are relatively lower than the corresponding results shown in Figure 2i. In Figure S2 (Supporting Information), the results of $g_{PIP2-PIP2}(r)$ in the system with PC:$PIP_2$ = 99:1 are similar to those shown in Figure 2. Figure S3 (Supporting Information) (PC:PS = 90:10) shows that, with the absence of the multivalent $PIP_2$ lipids, polyelectrolyte can also adsorb on the membrane with the pool of PS lipids. By increasing $C_i$, the polyelectrolyte desorbs from the membrane gradually.

### 3.3. Conformation Properties of the Polyelectrolyte.

The conformation of adsorbing polyelectrolyte on the charged membrane, which is controlled by the polyelectrolyte chain length $N$, charge density $Z_b$, and solution ionic strength $C_i$, is expected to be different from that of the polyelectrolyte in solution. We vary $N$ from 10 to 100 and set $Z_b$ as +1 and +2, respectively. The solution ionic concentration ranges from $C_i$ = 0.001 M ($\kappa^{-1} = 96$ Å) to $C_i = 1$ M ($\kappa^{-1} = 3$ Å). We define the corresponding critical Debye screening length of $C_i^C$ as $\kappa_C^{-1}$.

Figure 3a and b present the influences of charge density ($Z_b$) and chain length ($N$) of the polyelectrolyte as well as the $\kappa^{-1}$ of the solution on the parallel ($\langle R_g^2 \rangle_P$) and orthogonal ($\langle R_g^2 \rangle_O$) components of the mean-square radius of gyration, respectively. The composition of the membranes is PC:$PIP_2$ = 99:1. When $Z_b$ of polyelectrolyte is +1 (the solid symbols and solid lines) and $\kappa^{-1}$ is less than $\kappa_C^{-1}$, with the increase of $\kappa^{-1}$, random-coil-like polyelectrolyte becomes stretched with the increase of $\langle R_g^2 \rangle_P$ and $\langle R_g^2 \rangle_O$. By increasing $\kappa^{-1}$ to the critical adsorption/desorption limit $\kappa_C^{-1}$, polyelectrolyte begins to interact with the membrane and undergo a transformation with a significant


dx.doi.org/10.1021/jp310017j | J. Phys. Chem. B 2013, 117, 989−1002

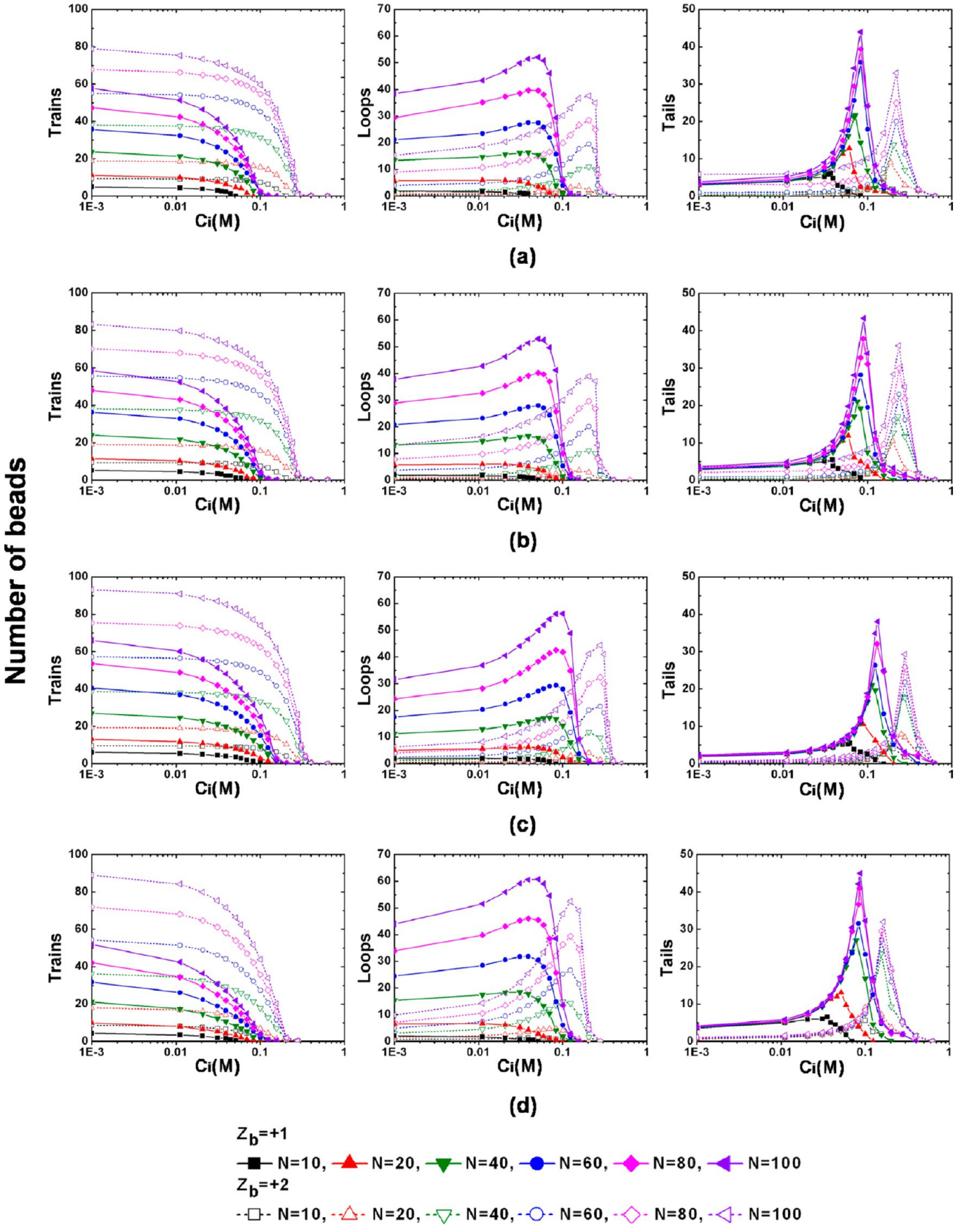


**Figure 4.** Number of beads in trains, loops, and tails of the polyelectrolytes as a function of $N$, $Z_b$, and $C_i$. The corresponding membrane compositions are PC:$PIP_2$ = 99:1 (a), PC:PS:$PIP_2$ = 98:1:1 (b), PC:PS:$PIP_2$ = 89:10:1 (c), and PC:PS=90:10 (d).


dx.doi.org/10.1021/jp310017j | J. Phys. Chem. B 2013, 117, 989−1002

increase of $\langle R_g^2\rangle_P$ and decrease of $\langle R_g^2\rangle_O$. When $\kappa^{-1} > \kappa_C^{-1}$, with the increase of $\kappa^{-1}$, polyelectrolyte becomes more stretched and closely adsorbed on the membrane, resulting in the further increase of $\langle R_g^2\rangle_P$ and decrease of $\langle R_g^2\rangle_O$. When $Z_b$ of polyelectrolyte is fixed as +2 (the vacant symbols and short dashed lines) and $\kappa^{-1}$ is smaller than $\kappa_C^{-1}$, electrostatic repulsion between beads becomes greatly enhanced; thus, $\langle R_g^2\rangle_P$ and $\langle R_g^2\rangle_O$ of the polyelectrolyte are quite larger than that of polyelectrolyte with $Z_b$ = +1. By increasing $\kappa^{-1}$ to $\kappa_C^{-1}$, stronger electrostatic interactions including attraction between polyelectrolyte beads and anionic lipids, electrostatic repulsion between beads, as well as electrostatic repulsion between anionic lipids cooperate to form smaller $\langle R_g^2\rangle_O$ and larger $\langle R_g^2\rangle_P$ than those of polyelectrolyte with $Z_b$ = +1. When $\kappa^{-1} > \kappa_C^{-1}$ and the total charge amount of polyelectrolyte exceeds that of the 25 $PIP_2$ lipids in the membrane ($N \geq 60$), the intrachain repulsion outweighs the attraction between the beads and the anionic lipids, leading to a significant increase of $\langle R_g^2\rangle_O$.

We also investigate the $\langle R_g^2\rangle_O$ and $\langle R_g^2\rangle_P$ variations of the polyelectrolytes adsorbing on membranes with composition of PC:PS:$PIP_2$ = 98:1:1, PC:PS:$PIP_2$ = 89:10:1, and PC:PS = 90:10. In Figure 3g and h, when the polyelectrolyte interacts with the pool of monovalent PS lipids in the membrane (PC:PS = 90:10), its total charge amount is not enough to neutralize PS lipids; therefore, for the adsorbing polyelectrolyte with $Z_b$ = +2 and $N \geq 60$, no significant increase of $\langle R_g^2\rangle_O$ (as shown in Figure 3b) is observed. $\langle R_g^2\rangle_P$ increases slightly for polyelectrolyte with $N \geq 60$, which is caused by the increasing electrostatic repulsion between an increasing number of adsorbing beads. When the polyelectrolyte adsorbs on the ternary mixed membrane with PC:PS:$PIP_2$ = 98:1:1 (Figure 3c and d), it interacts with the minor multivalent $PIP_2$ lipids preferentially. If the total charge amount of the polyelectrolyte is larger than that of $PIP_2$ lipids ($N \geq 60$ and $Z_b$ = +2), after segregation of all the $PIP_2$ lipids, the polyelectrolyte further interacts with monovalent PS lipids; thus, ($\langle R_g^2\rangle_O$) decreases compared with the corresponding results in Figure 3b. In the PC:PS:$PIP_2$ = 89:10:1 membrane (Figure 3e and f), more monovalent PS lipids can interact with the adsorbing polyelectrolyte with long chain length ($N \geq 60$) and high charge density ($Z_b$ = +2); therefore, when $\kappa^{-1} > \kappa_C^{-1}$, the corresponding $\langle R_g^2\rangle_O$ presents quite lower values than that of PC:PS:$PIP_2$ = 98:1:1 (Figure 3d).

We can conclude that, as the polyelectrolyte adsorbs on the charged membrane, its conformation exhibits a transition from three-dimensional random-coil-like to two-dimensional pancake-like chain and the polyelectrolyte flattens with decreased $\langle R_g^2\rangle_O$ and increased $\langle R_g^2\rangle_P$. Our calculation results of the separate parallel and orthogonal components of $\langle R_g^2\rangle$ show the influences of chain length and charge density of the polyelectrolyte, the membrane composition, as well as the $\kappa^{-1}$ ($C_i$) on the polyelectrolyte anisotropic variations, which accompany the adsorption/desorption process.

To further investigate the structure variations of the polyelectrolyte in the adsorption/desorption process, in Figure 4, we present the number of beads in trains, loops, and tails of the polyelectrolyte as a function of $N$, $Z_b$ and $C_i$.

Figure 4a shows the structure variation of the polyelectrolyte adsorbing on the lipid membrane with a composition of PC:$PIP_2$ = 99:1. When the charge density ($Z_b$) of polyelectrolyte is +1 (the solid symbols and solid lines) and $C_i$ is less than 0.01 M, the number of beads in trains and loops levels off. For short chains ($N \leq 20$), beads are mainly in trains and fewer beads are present in loops and tails. As $N$ increases (Figure 4a), the number of beads in trains and loops increases significantly, but the number of beads in tails only increases slightly. This is mainly because the mobile anionic lipids prohibit the formation of long tails; thus, the length of the tails cannot increase linearly with $N$. When $C_i$ is greater than 0.01 M, the electrostatic interaction is screened by the increasing solution ionic strength, allowing the membrane to attract less polyelectrolyte beads. By further increasing $C_i$ to the critical adsorption/desorption limit $C_i^C$, the number of beads in trains decreases while the number of beads in loops and tails increases to reach a maximum value. When $C_i > C_i^C$, polyelectrolyte desorbs and the number of beads in trains, loops, and tails decreases rapidly. When $Z_b$ is fixed as +2 (the vacant symbols and short dashed lines), the polyelectrolyte chain adsorbs onto the membrane more firmly, with more beads in trains compared with polyelectrolyte with the same chain length and low charge density ($Z_b$ = +1). When $C_i < 0.01$ M, short chains ($N \leq 40$) preferentially exhibit a tendency to flatten because this lowers the energy most. When the total charge amount of polyelectrolyte is larger than that of the 25 $PIP_2$ lipids in the membrane ($N \geq 60$), the polyelectrolyte protrudes into the solution and the bead numbers in loops and tails increase significantly. The relatively high charge density of the polyelectrolyte greatly enhances the adsorption interaction between beads and oppositely charged lipids; thus, the corresponding $C_i^C$ increases significantly. The stronger electrostatic attraction between polyelectrolyte and membrane limits the thermal movements of the beads; therefore, at higher $C_i^C$, the chain desorbs from the membrane with relatively smaller tails and loops than the polyelectrolyte with $Z_b$ of +1.

Figure 4b shows the number of beads in trains, loops of the polyelectrolyte adsorbing on membrane with PC:PS:$PIP_2$ = 98:1:1. The conformational variation tendencies of the chain are similar to those in Figure 4a, but as described in our previous discussion, the addition of 1% monovalent PS lipids in membrane can slightly improve the attraction between the polyelectrolyte and the membrane; thus, $C_i^C$ increases slightly. When $C_i < 0.01$ M, a few more beads are present in trains of the polyelectrolytes than the corresponding results in Figure 4a, and fewer beads are in loops and tails. For the polyelectrolyte with long chain length ($N \geq 60$) and high charge density ($Z_b$ = +2), monovalent anionic PS lipids can adsorb to neutralize the polyelectrolytes, leading to a fewer number of beads in tails than that in Figure 4a. By further increasing $C_i$ to $C_i^C$, the main adsorption/desorption behavior of the chains is similar to that in Figure 4a. Further, in Figure 4c, we present the detailed conformation variation of the polyelectrolyte adsorbing on membrane with the composition of PC:PS:$PIP_2$ = 89:10:1. With the addition of 10% monovalent anionic PS lipids in the membrane, the attraction between polyelectrolyte and the membrane enhances greatly. $C_i^C$ presents a significant increase, while the main adsorption/desorption behavior of the chains is similar to that shown in Figure 4a and b, with more polyelectrolyte beads present in trains when $C_i < C_i^C$, and more beads present in loops and less beads in tails at higher $C_i^C$ due to the stronger adhesion with more diffusing anionic lipids on the membrane.

Figure 4d shows that, on membrane with PC:PS = 90:10, the absence of 1% multivalent $PIP_2$ lipids significantly weakens the electrostatic attraction between membrane and polyelectrolytes. When $C_i < 0.01$ M, fewer beads are present in trains than the corresponding results in Figure 4c, whereas more are present in


dx.doi.org/10.1021/jp310017j | J. Phys. Chem. B 2013, 117, 989−1002

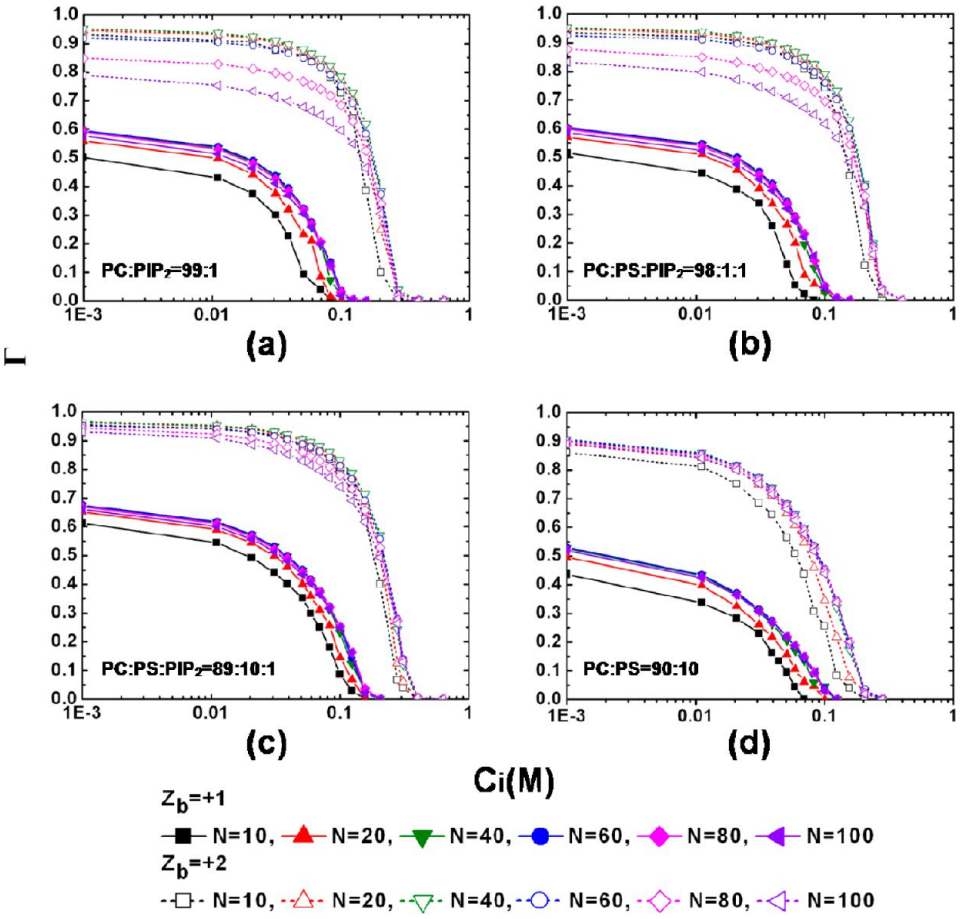


**Figure 5.** Adsorption amount Γ of the polyelectrolyte as a function of $N$, $Z_b$, and $C_i$. The membrane compositions are PC:$PIP_2$ = 99:1 (a), PC:PS:$PIP_2$ = 98:1:1 (b), PC:PS:$PIP_2$ = 89:10:1 (c), and PC:PS=90:10 (d).

loops and tails. As $C_i$ increases to $C_i^C$, more beads are present in loops and tails at lower $C_i^C$, compared to the results in Figure 4c.

**3.4. Adsorption Amount of the Polyelectrolyte and Surface Converge of the Membrane.** We further explore the adsorption properties of polyelectrolytes by detecting the adsorption amount (Γ) of the polyelectrolyte and the membrane surface coverage ($\theta$). Figure 5a shows the variation of Γ against the charge density ($Z_b$) and chain length ($N$) of the polyelectrolyte as well as the solution ionic strength ($C_i$), and the membrane compositions are PC:$PIP_2$ = 99:1. When 0.001 M < $C_i$ < $C_i^C$ and $Z_b$ is +1, with the increase of $N$ from 10 to 60, the stronger cooperativity effect of the beads in longer polyelectrolyte enhances its adsorption on the membrane; thus, Γ increases. With the further increase of $N$, Γ decreases slightly, which is the result of the competition between the adsorption energy gain and the conformational entropy loss. When $Z_b$ is fixed as +2, at low ionic strength ($C_i$ < 0.01 M), the chain adsorbs on the membrane surface more firmly, with Γ significantly increasing to more than 0.8 compared with 0.5 for polyelectrolyte with the same chain length and low charge density (+1). When $N$ = 40, Γ reaches a maximum value in the range of 0.001 M < $C_i$ < $C_i^C$ . As $N$ > 60, the total charge amount of the polyelectrolyte is larger than the total charge amount of the 25 $PIP_2$ lipids on the membrane, leading to the stronger repulsion interaction between beads; thus, with the further increase of $N$, Γ decreases dramatically. In Figure 5a, by further increasing $C_i$, the polyelectrolyte desorption occurs and Γ decreases. Figure 5d shows that, on membrane with PC:PS = 90:10, the total charge amount of the polyelectrolyte is not enough to neutralize PS lipids; therefore, for polyelectrolyte with $Z_b$ = +2, no significant Γ decrease due to electrostatic repulsion between beads (as shown in Figure 4a) is observed. When $N$ > 60, the competition between gain of adsorption energy and conformational entropy loss only results in a slight decrease of Γ. Figure 5b and c show Γ of polyelectrolyte adsorbing on the membrane with PC:PS:$PIP_2$ = 98:1:1 and PC:PS:$PIP_2$ = 89:10:1, respectively. The polyelectrolyte ($N$ > 60, $Z_b$ = +2) whose total charge amount of the polyelectrolyte exceeds that of $PIP_2$ lipids further attracts monovalent PS lipids; thus, Γ increases compared with the corresponding results in Figure 5a.

We show changes of membrane surface coverage $\theta$ as a function of chain length and charge density of the polyelectrolyte as well as ionic strength in Figure 6. $\theta$ monotonically decreases with $C_i$ and increases with $N$, $Z_b$ of the polyelectrolyte, which illustrates that membrane surface coverage is a monotonic function of $Z_b$, $N$, and $C_i$.

**3.5. Overcharging of the Membrane.** We further calculate the "electronic adsorption amount", $\Gamma_e$ (see eq 12). Figure 7 shows that, with the increase of the $N$ and $Z_b$ as well as the decrease of $C_i$, $\Gamma_e$ increases significantly. In Figure 7a and b, the adsorbing polyelectrolytes with long chain length and large charge density can overcharge the membrane by providing more cations to the membrane surface than is necessary to neutralize anionic lipids ($\Gamma_e$ > 1); thus, the charge inversion of


dx.doi.org/10.1021/jp310017j | J. Phys. Chem. B 2013, 117, 989−1002

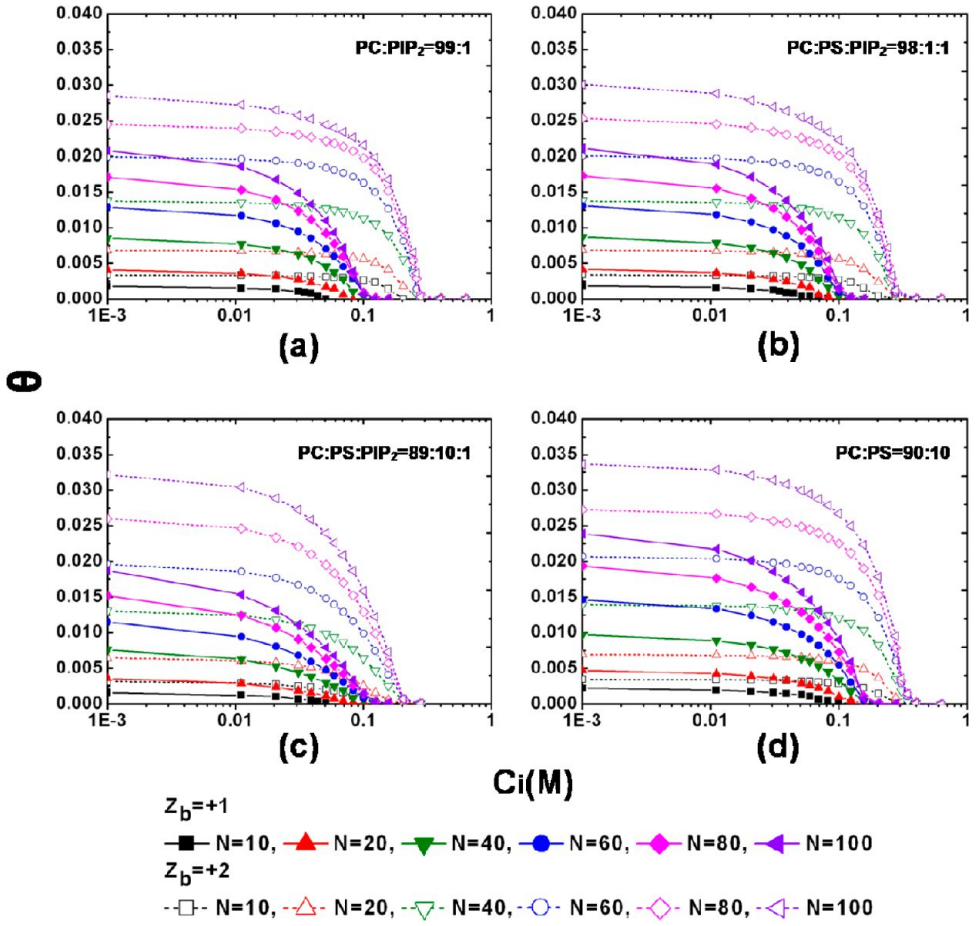


**Figure 6.** Membrane surface coverage $\theta$ as a function of $N$, $Z_b$, and $C_i$. The membrane compositions are PC:$PIP_2$ = 99:1 (a), PC:PS:$PIP_2$ = 98:1:1 (b), PC:PS:$PIP_2$ = 89:10:1 (c), and PC:PS=90:10 (d).

the membrane occurs. As a result, the overcharged membrane would attract other negatively charged membrane, which is distinct evidence for the bridging effect of the charged biomacromolecules for membranes.

## 4. CONCLUSION

In this work, we employ Monte Carlo simulations to investigate the nonspecific electrostatic adsorption between a cationic flexible polyelectrolyte and an impenetrable, fluid mixed lipid membrane containing different anionic lipid species. We investigate the adsorption/desorption limit and explore the polyelectrolyte conformational changes as well as the membrane lipid redistribution by focusing on the influence of polyelectrolyte chain length and charge density, solution ionic concentration, and membrane composition. The findings are as follows:

(A) Adsorption occurs if the gain of system energy can compensate the loss of the polyelectrolyte chain conformational entropy and anionic lipid demixing entropy. Longer chain length, higher charge density of polyelectrolyte, and presence of $PIP_2$ lipids and large number of PS lipids in the membrane lead to higher adsorption/desorption critical limit $C_i^C$.

(B) On the binary mixed membrane, the adsorbing polyelectrolyte can effectively cluster the anionic lipids. On the ternary mixed membrane, the multivalent lipids preferentially bind around the polyelectrolyte and competitively inhibit the binding of the monovalent lipids, When the total charge amount of the polyelectrolyte exceeds that of the local $PIP_2$ lipids, it can further attract monovalent PS lipids around the polyelectrolyte/$PIP_2$ complex.

(C) The solution ionic strength influences the tendency of the polyelectrolyte adsorption, chain conformational properties, and anionic lipid distribution. At low ionic strength ($C_i$), charge screening is negligible and electrostatic attractions between the membrane and chain cause the polyelectrolyte to adsorb and flatten onto the membrane with anionic lipid clustering. As the ionic strength increases, the screening effect weakens the polyelectrolyte/membrane electrostatic attractions, and the number of adsorbing chain beads as well as the anionic lipid segregation extent decrease. When $C_i > C_i^C$, by further increasing the ionic strength, the polyelectrolyte chain desorbs from the membrane and presents a flexible-coil conformation in the solution, and the anionic lipid segregation disappears.

(D) Polyelectrolytes with low bead charge density (+1) adsorb through attachment of relatively fewer beads to the membrane surface, while other beads are involved in the loops and tails. By increasing the chain length, more beads are adsorbing on the membrane, and more anionic lipids are bound. The responsive diffusing anionic lipids prohibit the polyelectrolyte chain from forming too long tails. Polyelectrolytes with higher charge density (+2) adsorb on the membrane more firmly, and the polyelectrolytes with longer chain length can overcharge the membranes with low charge density. Electrostatic repulsion prohibits additional bead adsorption on the membrane, and extended loops and tails of the chains are formed in solution. The number of adsorbed


dx.doi.org/10.1021/jp310017j | J. Phys. Chem. B 2013, 117, 989−1002

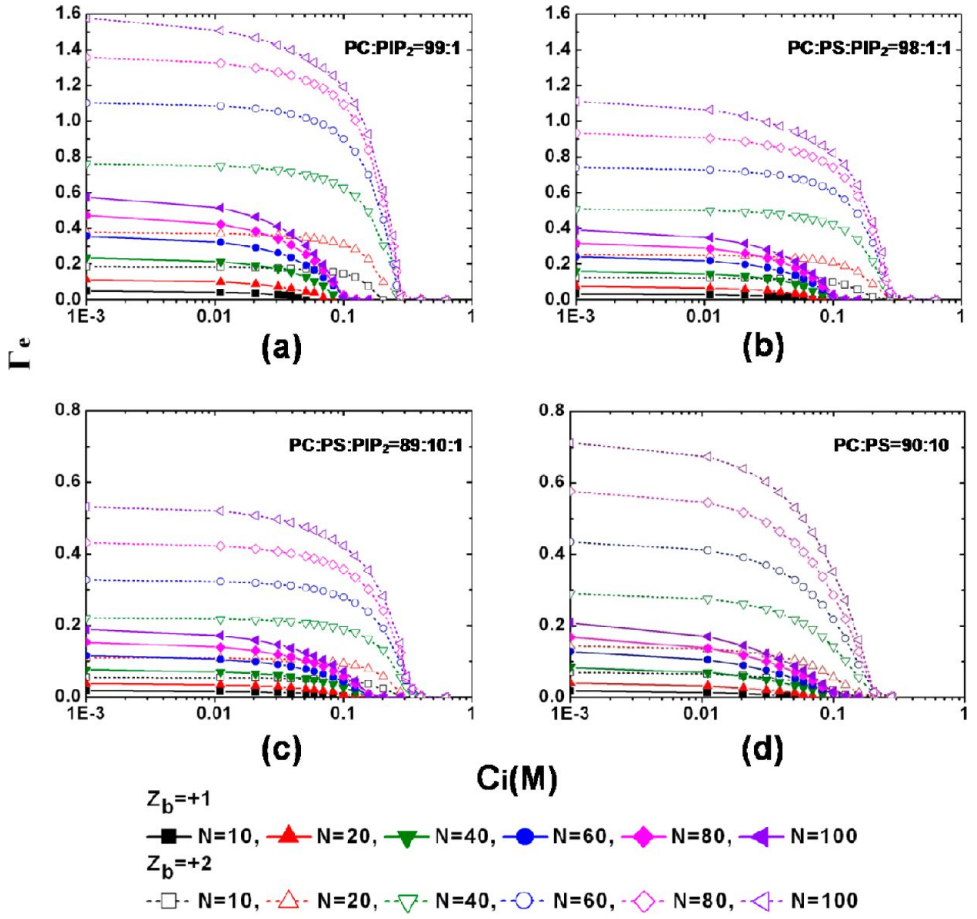


**Figure 7.** Electronic adsorption amount $\Gamma_e$ of the polyelectrolyte as a function of $N$, $Z_b$, and $C_i$. The membrane compositions are PC:$PIP_2$ = 99:1 (a), PC:PS:$PIP_2$ = 98:1:1 (b), PC:PS:$PIP_2$ = 89:10:1 (c), and PC:PS=90:10 (d).

polyelectrolyte chain beads also increases with the increase of membrane surface charge density.

We hope our systematical investigation can provide further inspiration for structure studies of the polyelectrolyte/membrane complex in realistic systems, and is helpful for selecting an appropriate polyelectrolyte or biomacromolecule for applications such as anionic lipid regulation.

## ■ ASSOCIATED CONTENT

### Supporting Information

The radial distribution functions (RDFs) of each lipid species in the membrane with lipid compositions of PC:PS:$PIP_2$ = 89:10:1, PC:$PIP_2$ = 99:1, and PC:PS:$PIP_2$ = 90:10. This material is available free of charge via the Internet at http://pubs.acs.org.

## ■ AUTHOR INFORMATION

### Corresponding Author

*E-mail: tfshi@ciac.jl.cn. Phone: +86-431-85262309. Fax: +86-431-85262969.

### Notes

The authors declare no competing financial interest.

## ■ ACKNOWLEDGMENTS

This work is supported by the National Natural Science Foundation of China (51028301) Programs and the Fund for Creative Research Groups (50921062), and subsidized by the Special Funds for National Basic Research Program of China (2009CB930100).

## ■ REFERENCES

(1) McLaughlin, S.; Murray, D. *Nature* **2005**, *438*, 605−611.
(2) Heo, W. D.; Inoue, T.; Park, W. S.; Kim, M. L.; Park, B. O.; Wandless, T. J.; Meyer, T. *Science* **2006**, *314*, 1458−1461.
(3) Yeung, T.; Gilbert, G. E.; Shi, J.; Silvius, J.; Kapus, A.; Grinstein, S. *Science* **2008**, *319*, 210−213.
(4) Di Paolo, G.; De Camilli, P. *Nature* **2006**, *443*, 651−657.
(5) Lemmon, M. A. *Traffic* **2003**, *4*, 201−213.
(6) Czech, M. P. *Cell* **2000**, *100*, 603−606.
(7) Mitrakos, P.; Macdonald, P. M. *Biomacromolecules* **2000**, *1*, 365−376.
(8) Gambhir, A.; Hangyas-Mihalyne, G.; Zaitseva, I.; Cafiso, D. S.; Wang, J. Y.; Murray, D.; Pentyala, S. N.; Smith, S. O.; McLaughlin, S. *Biophys. J.* **2004**, *86*, 2188−2207.
(9) Murray, D.; Arbuzova, A.; Honig, B.; McLaughlin, S. *Curr. Top. Membr.* **2002**, *52*, 277−307.
(10) Porcar, I.; Garcia, R.; Gomez, C.; Campos, A.; Abad, C. *Polymer* **1997**, *38*, 5107−5113.
(11) Porcar, I.; Garcia, R.; Soria, V.; Campos, A. *Polymer* **1997**, *38*, 3545−3552.
(12) Porcar, I.; Garcia, R.; Soria, V.; Campos, A. *Polymer* **1997**, *38*, 3553−3560.
(13) Porcar, I.; Gomez, C. M.; Perezpaya, E.; Soria, V.; Campos, A. *Polymer* **1994**, *35*, 4627−4637.
(14) deMeijere, K.; Brezesinski, G.; Mohwald, H. *Macromolecules* **1997**, *30*, 2337−2342.
(15) Raudino, A.; Castelli, F. *Macromolecules* **1997**, *30*, 2495−2502.

(16) Rusu, L.; Gambhir, A.; McLaughlin, S.; Radler, J. *Biophys. J.* **2004**, *87*, 1044−1053.
(17) Golebiewska, U.; Nyako, M.; Woturski, W.; Zaitseva, I.; McLaughlin, S. *Mol. Biol. Cell* **2008**, *19*, 1663−1669.
(18) Wang, J. Y.; Gambhir, A.; Hangyas-Mihalyne, G.; Murray, D.; Golebiewska, U.; McLaughlin, S. *J. Biol. Chem.* **2002**, *277*, 34401−34412.
(19) Dietrich, U.; Kruger, P.; Gutberlet, T.; Kas, J. A. *Biochim. Biophys. Acta, Biomembr.* **2009**, *1788*, 1474−1481.
(20) Wu, C. M.; Liou, W.; Chen, H. L.; Lin, T. L.; Jeng, U. S. *Macromolecules* **2004**, *37*, 4974−4980.
(21) Goldenberg, N. M.; Steinberg, B. E. *Cancer Res.* **2010**, *70*, 1277−1280.
(22) Cai, X. M.; Lietha, D.; Ceccarelli, D. F.; Karginov, A. V.; Rajfur, Z.; Jacobson, K.; Hahn, K. M.; Eck, M. J.; Schaller, M. D. *Mol. Cell. Biol.* **2008**, *28*, 201−214.
(23) Cicchetti, G.; Biernacki, M.; Farquharson, J.; Allen, P. G. *Biochemistry* **2004**, *43*, 1939−1949.
(24) Sarkar, J.; Annepu, H.; Sharma, A. *J. Adhes.* **2011**, *87* (3), 214−234.
(25) Yan, H. D.; Villalobos, C.; Andrade, R. *J. Neurosci.* **2009**, *29*, 10038−10046.
(26) Yeh, L. H.; Xue, S.; Joo, S. W.; Qian, S.; Hsu, J. P. *J. Phys. Chem. C* **2012**, *116*, 4209−4216.
(27) Ferguson, C. G.; James, R. D.; Bigman, C. S.; Shepard, D. A.; Abdiche, Y.; Katsamba, P. S.; Myszka, D. G.; Prestwich, G. D. *Bioconjugate Chem.* **2005**, *16*, 1475−1483.
(28) Mollapour, M.; Phelan, J. P.; Millson, S. H.; Piper, P. W.; Cooke, F. T. *Biochem. J.* **2006**, *395*, 73−80.
(29) Santin, M.; Rhys-Williams, W.; O'Reilly, J.; Davies, M. C.; Shakesheff, K.; Love, W. G.; Lloyd, A. W.; Denyer, S. P. *J. R. Soc., Interface* **2006**, *3*, 277−281.
(30) Im, Y. J.; Perera, I. Y.; Brglez, I.; Davis, A. J.; Stevenson-Paulik, J.; Phillippy, B. Q.; Johannes, E.; Allen, N. S.; Boss, W. F. *Plant Cell* **2007**, *19*, 1603−1616.
(31) Honda, A.; Nogami, M.; Yokozeki, T.; Yamazaki, M.; Nakamura, H.; Watanabe, H.; Kawamoto, K.; Nakayama, K.; Morris, A. J.; Frohman, M. A.; et al. *Cell* **1999**, *99*, 521−532.
(32) Tall, E. G.; Spector, I.; Pentyala, S. N.; Bitter, I.; Rebecchi, M. J. *Curr. Biol.* **2000**, *10*, 743−746.
(33) Watt, S. A.; Kular, G.; Fleming, I. N.; Downes, C. P.; Lucocq, J. M. *Biochem. J.* **2002**, *363*, 657−666.
(34) McLaughlin, S.; Wang, J. Y.; Gambhir, A.; Murray, D. *Annu. Rev. Biophys. Biomol. Struct.* **2002**, *31*, 151−175.
(35) Bazzi, M. D.; Nelsestuen, G. L. *Biochemistry* **1991**, *30*, 7961−7969.
(36) Golebiewska, U.; Gambhir, A.; Hangyas-Mihalyne, G.; Zaitseva, I.; Radler, J.; McLaughlin, S. *Biophys. J.* **2006**, *91*, 588−599.
(37) Tian, W. D.; Ma, Y. Q. *Soft Matter* **2012**, *8*, 6378−6384.
(38) Dias, R. S.; Linse, P. *Biophys. J.* **2008**, *94*, 3760−3768.
(39) Tzlil, S.; Ben-Shaul, A. *Biophys. J.* **2005**, *89*, 2972−2987.
(40) Dias, R. S.; Pais, A.; Linse, P.; Miguel, M. G.; Lindman, B. *J. Phys. Chem. B* **2005**, *109*, 11781−11788.
(41) Haleva, E.; Ben-Tal, N.; Diamant, H. *Biophys. J.* **2004**, *86*, 2165−2178.
(42) Loew, S.; Hinderliter, A.; May, S. *J. Chem. Phys.* **2009**, *130*, 045102.
(43) Mbamala, E. C.; Ben-Shaul, A.; May, S. *Biophys. J.* **2005**, *88*, 1702−1714.
(44) Khelashvili, G.; Weinstein, H.; Harries, D. *Biophys. J.* **2008**, *94*, 2580−2597.
(45) Cortese, J. D.; Voglino, A. L.; Hackenbrock, C. R. *J. Cell Biol.* **1991**, *113*, 1331−1340.
(46) Wang, L.; Liang, H. J.; Wu, J. Z. *J. Chem. Phys.* **2010**, *133*, 044906.
(47) Tzlil, S.; Murray, D.; Ben-Shaul, A. *Biophys. J.* **2008**, *95*, 1745−1757.
(48) Metropolis, N.; Rosenbluth, A. W.; Rosenbluth, M. N.; Teller, A. H.; Teller, E. *J. Chem. Phys.* **1953**, *21*, 1087−1092.
(49) Kawasaki, K. In *Phase Transitions and Critical Phenomena*; Domb, C., Green, M. S., Eds.; Academic Press: New York, 1972; Vol. 2.
(50) Jan, N.; Lookman, T.; Pink, D. A. *Biochemistry* **1984**, *23*, 3227−3231.
(51) Zhang, R.; Shi, T. F.; An, L. J.; Sun, Z. Y.; Tong, Z. *J. Phys. Chem. B* **2010**, *114*, 3449−3456.
(52) Chodanowski, P.; Stoll, S. *Macromolecules* **2001**, *34*, 2320−2328.